Mantle Shear-Wave Velocity Structure Beneath the Hawaiian Hot Spot

Cecily J. Wolfe *et al.*

Science **326**, 1388 (2009);
DOI: 10.1126/science.1180165

Science (print ISSN 0036-8075; online ISSN 1095-9203) is published weekly, except the last week in December, by the American Association for the Advancement of Science, 1200 New York Avenue NW, Washington, DC 20005.

Mantle Shear-Wave Velocity Structure Beneath the Hawaiian Hot Spot

Cecily J. Wolfe,[1]* Sean C. Solomon,[2] Gabi Laske,[3] John A. Collins,[4] Robert S. Detrick,[4] John A. Orcutt,[3] David Bercovici,[5] Erik H. Hauri[2]

Defining the mantle structure that lies beneath hot spots is important for revealing their depth of origin. Three-dimensional images of shear-wave velocity beneath the Hawaiian Islands, obtained from a network of sea-floor and land seismometers, show an upper-mantle low-velocity anomaly that is elongated in the direction of the island chain and surrounded by a parabola-shaped high-velocity anomaly. Low velocities continue downward to the mantle transition zone between 410 and 660 kilometers depth, a result that is in agreement with prior observations of transition-zone thinning. The inclusion of *SKS* observations extends the resolution downward to a depth of 1500 kilometers and reveals a several-hundred-kilometer-wide region of low velocities beneath and southeast of Hawaii. These images suggest that the Hawaiian hot spot is the result of an upwelling high-temperature plume from the lower mantle.

Hawaii is the archetypal hot spot and has been suggested to be the surface expression of a mantle plume: a localized upwelling of hot buoyant material from Earth's deep mantle (*1*, *2*), although such an origin has been debated. The Hawaiian-Emperor chain of islands and seamounts spans thousands of kilometers; records age-progressive volcanism for >75 million years (*3*); and exhibits a broad ~1000-km-wide region of elevated topography, known as the Hawaiian Swell (Fig. 1A), that surrounds the locus of current volcanism. Estimated to transport a larger buoyancy flux than any other active plume (*4*, *5*), the Hawaiian hot spot has been the focus of numerous geochemical and geodynamical studies [for example, (*4*–*10*)] that attempted to resolve its origin. One of the most straightforward indications of whether a hot spot is the result of a plume is the presence of a narrow, vertically continuous zone of low seismic velocities in the underlying mantle, indicative of higher-than-normal temperatures, anomalous mantle composition, or melt (*11*, *12*).

Global seismic tomography suggests that low seismic velocities may extend from the upper to the lower mantle beneath the Hawaiian hot spot (*13*–*15*), but there remains doubt about how well, and to what depth, narrow plumes may be resolved by such methods (*16*, *17*). Moreover, global models of mantle structure are limited in their resolution near Hawaii by the sparseness of wave paths, given the lack of seismic stations on the ocean floor and the great distances between the islands and most circum-Pacific earthquake sources. Previous investigations of mantle structure near Hawaii using island stations (*18*–*20*) or sea-floor deployments of instruments (*21*, *22*) have been limited in geographic coverage and numbers of instruments. Such experiments have not yielded the high-resolution regional tomographic models needed to settle the debate over even such a basic question as whether the upper mantle beneath the Hawaiian Islands is marked by low seismic velocities and higher-than-normal temperatures, as suggested by some studies (*13*–*15*, *19*), or not, as implied by others [for example, (*23*)].

Here we report results from the Hawaiian Plume-Lithosphere Undersea Melt Experiment (PLUME), which was designed to determine at high resolution the mantle seismic velocity structure beneath the Hawaiian hot spot, to assess the hypothesis that the hot spot is the product of an upwelling plume, and to determine how mantle flow may interact with the overlying lithosphere to generate the Hawaiian Swell. The experiment featured a dense, large-aperture seismic network consisting of two year-long deployments of three dozen broadband ocean-bottom seismometers (OBSs) and the concurrent deployment of 10 portable broadband seismometers on the Hawaiian Islands (Fig. 1A), with all instruments operating continuously to record teleseismic and local earthquakes. During the experiment period, 2146 *S*-wave relative arrival times (direct *S* and *SKS* phases) were collected from 97 earthquakes (*24*) (fig. S1) and corrected for estimated variations in station elevation and crustal thickness. Corrected mean station delay patterns reflect upper-mantle heterogeneity and indicate relatively low velocities beneath and to the west of the Hawaiian Islands and high velocities east of Hawaii and at distant stations around the margins of the swell (Fig. 1B).

The arrival times were inverted for *S*-wave velocity heterogeneity, damped earthquake relocations, and origin time terms using finite-frequency (*13*, *25*) methods. Because of the large station spacing, crossing wave paths were lacking, and vertical resolution was limited in the uppermost mantle. One strategy to mitigate the effect of smearing strong, shallow heterogeneity deeper into a model is to include station terms to partially absorb the effect of shallow structure, but this approach comes at the expense of decreased resolution at shallow depths, and tests indicate that station terms may not successfully absorb structure at depths of 100 to 200 km if such variations are extremely strong. We therefore performed inversions both with (Fig. 2 and fig. S6) and without (Fig. 2 and figs. S7 and S8) station terms. In both cases, a low-velocity anomaly was well resolved in the upper mantle beneath Hawaii and was elongated in a southeast-northwest direction parallel to the Hawaiian Islands. As expected, the

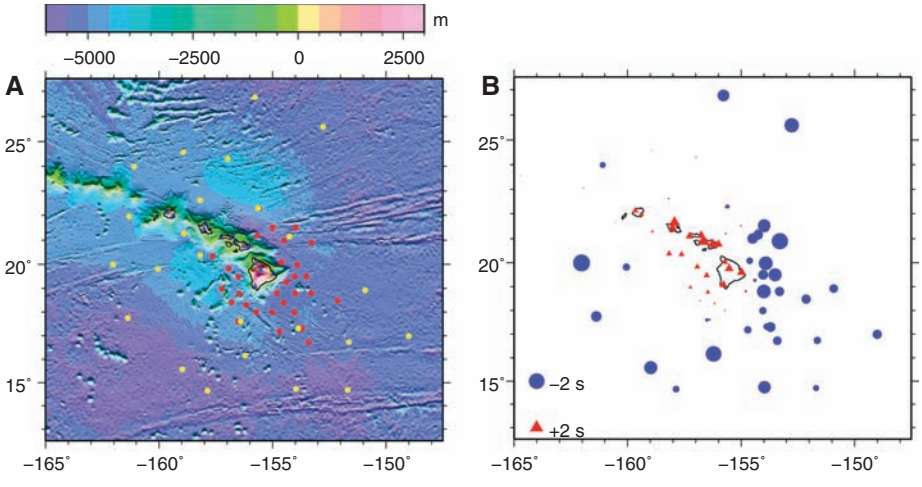

Fig. 1. (**A**) Locations of seismometers used in *S*-wave tomography. Land stations are indicated by blue triangles and OBSs are indicated by red (first deployment; 2005 to 2006) or yellow (second deployment; 2006 to 2007) circles. Only stations that successfully recorded two horizontal components are shown. Bathymetry is taken from (*30*). (**B**) Corrected mean station delays, adjusted to vertical incidence. Early arrivals are shown by blue circles and late arrivals by red triangles, with symbol size scaled linearly to the magnitude of the delay (see scale at lower left).

[1]Hawaii Institute of Geophysics and Planetology, University of Hawaii at Manoa, Honolulu, HI 96822, USA. [2]Department of Terrestrial Magnetism, Carnegie Institution of Washington, Washington, DC 20015, USA. [3]Cecil H. and Ida M. Green Institute of Geophysics and Planetary Physics, Scripps Institution of Oceanography, San Diego, CA 92093, USA. [4]Woods Hole Oceanographic Institution, Woods Hole, MA 02543, USA. [5]Department of Geology and Geophysics, Yale University, New Haven, CT 06520, USA.

*To whom correspondence should be addressed. E-mail: cecily@soest.hawaii.edu

amplitude of upper-mantle heterogeneity was larger in inversions without station terms. A parabola-shaped region of higher-than-average seismic velocity along the edge of the Hawaiian Swell was also observed to extend downward to 300 km depth, although patterns outside its boundaries were constrained only to the southeast, where station coverage extends beyond its edge. Low velocities beneath Hawaii continue into the transition zone, and inversions resolved a broad region of low velocities in the lower mantle from 700 to 1500 km depth southeast of Hawaii (Fig. 3).

The vertical extent of upper mantle structure is not well constrained by our *S*-wave data alone, as illustrated by a two-step inversion (fig. S9). In the first step, we inverted for a model in which all structure was "squeezed" between 50 and 250 km depth. In the second step, we corrected the observations for the effects of the squeezed model and inverted for an additional residual model. The two-step model continued to recover a low-velocity anomaly in the transition zone, and the model deeper than 500 km remained virtually unchanged, but much of the heterogeneity at 300 km depth can be squeezed to shallower depths. Given the tradeoffs between the amplitude and the depth interval of heterogeneity, however, lateral variations at 100 to 200 km depth in this two-step model were extremely large at ±8%. Although reconciliation with surface-wave observations is needed to provide firm limits on the lateral variation in upper-mantle seismic velocities and help resolve these ambiguities, prior surface-wave observations (*21*) and analysis of PLUME data to date indicate mantle *S*-wave velocity heterogeneity of no more than ±4% in the depth interval from 60 to 140 km and are thus inconsistent with the large variations recovered in the two-step model.

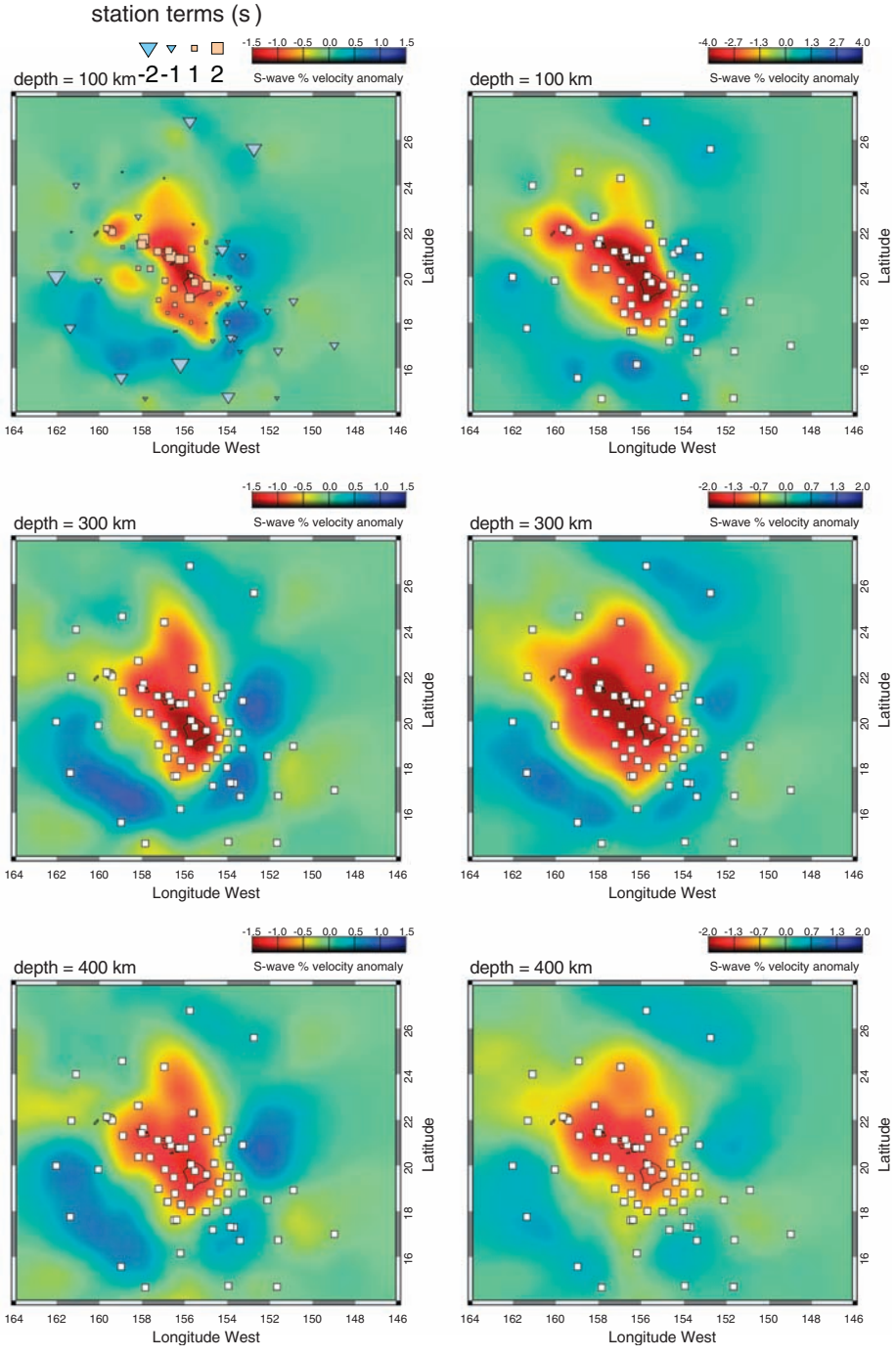

Fig. 2. Upper-mantle velocity heterogeneity at (**top**) 100, (**middle**) 300, and (**bottom**) 400 km depth. The scale of heterogeneity is indicated in the upper right corner of each panel. The left column displays solutions from an inversion with station terms; the right column shows the results of an inversion without station terms.

SKS waves have steeper arrival angles than direct *S* waves do and thus provide wave paths that sample the lower mantle beneath Hawaii (fig. S2). To test how the subset of *SKS* data contributes to the resolution of lower-mantle structure, we performed inversions in which *SKS* phases were excluded (figs. S11 and S12). Direct *S* waves from the first deployment dominantly constrained the low-velocity anomaly in the upper mantle beneath and around the main Hawaiian Islands, but these inversions had less structure in the mantle transition zone (410 to 660 km depth) and negligible lower mantle structure (fig. S11). Including direct *S*-wave data from the second OBS deployment extended the spatial region of the model and improved resolution of the low-velocity anomaly in the upper mantle and transition zone (fig. S12), but lower-mantle heterogeneity remained small. These tests indicate that low velocities in the lower mantle beneath Hawaii are not artifacts of vertical smearing of strong upper-mantle heterogeneity, but instead are driven by the resolving power of *SKS* arrival times. The existence and southeastern position of the lower-mantle anomaly constrained by *SKS* data were affected, however, by the solution for shallower upper-mantle structure (*24*). Heterogeneity deeper than 1500 km is not required by our data alone, but the eventual incorporation of PLUME data into global models may extend the resolution to greater depths. Montelli *et al.* (*13*, *14*) imaged a broad region of low velocities beneath Hawaii that extended downward to 1900 km depth in their global *S*-wave model and to the core/mantle boundary in their *P*-wave model. Our low-velocity anomaly is narrower than the ~10°-wide anomaly displayed by Montelli *et al.* (*13*, *14*), which is probably an indication of the improved horizontal resolution provided by the PLUME data. Resolution tests conducted with a wide variety of cylindrical and checkerboard structures (figs. S16 to S28) demonstrate that the PLUME data set resolves both upper- and lower-mantle structure at the level of our interpretations. One possible biasing effect on our solutions in the lower mantle, however, may come from undetermined structure near the core/mantle boundary

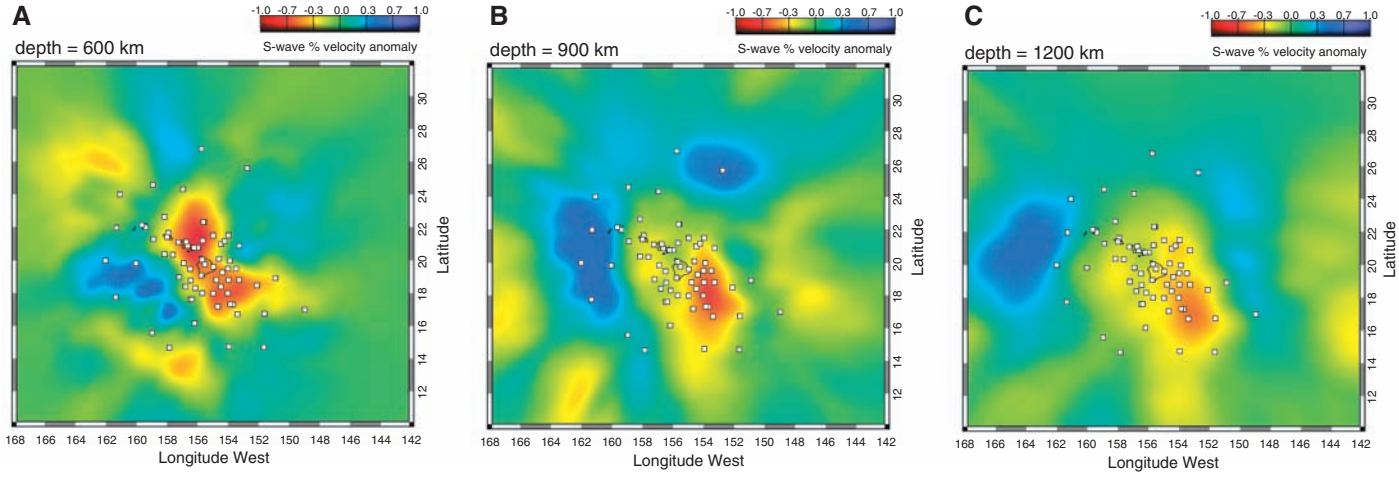

Fig. 3. Velocity heterogeneity (without station terms) at (**A**) 600, (**B**) 900, and (**C**) 1200 km depth.

(*24*), where steep lateral velocity gradients have been observed at the edges of the Pacific large low-shear-velocity province (*26*).

Our results improve the fidelity of *S*-wave mantle imaging around Hawaii as compared with previous efforts and suggest that the upper mantle beneath the islands is characterized by low seismic velocities and, by inference, anomalously high temperatures. The peak-to-peak 3% velocity variations that we imaged at 300 km depth in inversions with station terms corresponds to a temperature variation across the model of 250°C, and the 1.5% contrast near 900 km depth corresponds to a temperature variation of 300°C (*24*). These values are consistent with prior petrologic and geodynamic inferences of a high-temperature plume beneath the Hawaiian hot spot (*4*–*6*, *10*, *27*).

In terms of plume dynamics, the broad, low-velocity anomaly at shallow mantle depths (<200 km) beneath the islands (Figs. 1 and 2) is in agreement with the prediction from geodynamic models of a "pancake" of high-temperature material as the plume impacts and spreads laterally beneath the rigid lithosphere. Some geodynamic models (*6*, *10*) also predict a parabola-shaped curtain of cold downwelling material that isolates plume flow from the surrounding mantle, which is consistent with the parabola-shaped volume of high upper-mantle velocities imaged in our models. Delay patterns display asymmetry around the island of Hawaii (Fig. 1), with greater delays in the western offshore region between Hawaii and Maui (where bathymetry is correspondingly shallower) and earlier arrivals to the east (where the sea floor is deeper). These coupled characteristics of seismic velocity and sea-floor topography probably reflect three-dimensional complexities in uppermost mantle flow and melting (*10*) and provide constraints for improving geodynamic models to resolve finer details of how shallow mantle flow generates uplift and magmatism.

At greater depths, velocity heterogeneity (±1%) within the mantle transition zone is consistent with prior observations of transition-zone thinning along the island chain (*20*, *22*), interpreted as reflecting higher-than-normal temperatures. Although a thermal boundary layer near the base of the transition zone has been suggested as a candidate source region for some plumes, our images display low velocities continuing into the lower mantle, suggesting that the source region for the Hawaiian plume is at still greater depth in the lower mantle. The southeastern location of the center of low velocities is consistent with geodynamic arguments that plume conduits may be tilted by advection within a large-scale mantle flow field (*28*), and the large horizontal aperture of the anomaly is in agreement with predictions that a plume may be wider in the lower mantle because of greater viscosity than in the upper mantle (*29*).

Because Hawaiian lavas are chemically distinct (*7*–*9*) from mid-ocean ridge basalts, both temperature and compositional variations may also contribute to seismic heterogeneity, and the geodynamic characteristics of thermochemical plumes can deviate from the classic features of thermal plumes (*12*). Nonetheless, many aspects of the *S*-wave images derived from the PLUME observations conform to the expected signatures of the mantle plume model.

References and Notes

1. J. T. Wilson, *Can. J. Phys.* **42**, 893 (1963).
2. W. J. Morgan, *Nature* **230**, 42 (1971).
3. R. A. Duncan, R. A. Keller, *Geochem. Geophys. Geosyst.* **5**, Q08L03 (2004).
4. G. F. Davies, *J. Geophys. Res.* **93**, 10467 (1988).
5. N. H. Sleep, *J. Geophys. Res.* **95**, 6715 (1990).
6. N. M. Ribe, U. R. Christensen, *J. Geophys. Res.* **99**, 669 (1994).
7. E. H. Hauri, *Nature* **382**, 415 (1996).
8. A. V. Sobolev, A. W. Hofmann, S. V. Sobolev, I. K. Nikogosian, *Nature* **434**, 590 (2005).
9. M. D. Kurz, W. J. Jenkins, S. R. Hart, D. Clague, *Earth Planet. Sci. Lett.* **66**, 388 (1983).
10. W. B. Moore, G. Schubert, P. Tackley, *Science* **279**, 1008 (1998).
11. V. Courtillot, A. Davaille, J. Besse, J. Stock, *Earth Planet. Sci. Lett.* **205**, 295 (2003).
12. G. Ito, P. E. van Keken, in *Mantle Dynamics*, D. Bercovici, Ed., *Treatise on Geophysics* (Elsevier, New York, 2007), vol. 7, pp. 371–435.
13. R. Montelli *et al.*, *Science* **303**, 338 (2004).
14. R. Montelli, G. Nolet, F. A. Dahlen, G. Masters, *Geochem. Geophys. Geosyst.* **7**, Q11007 (2006).
15. C. Li, R. D. van der Hilst, E. R. Engdahl, S. Burdick, *Geochem. Geophys. Geosyst.* **9**, Q05018 (2008).
16. R. D. van der Hilst, M. V. de Hoop, *Geophys. J. Int.* **163**, 956 (2005).
17. L. Boschi, T. W. Becker, G. Soldati, A. M. Dziewonski, *Geophys. Res. Lett.* **33**, L06302 (2006).
18. X. Li *et al.*, *Nature* **405**, 938 (2000).
19. C. J. Wolfe, S. C. Solomon, P. G. Silver, R. M. Russo, J. C. VanDecar, *Earth Planet. Sci. Lett.* **198**, 129 (2002).
20. Y. Shen, C. J. Wolfe, S. C. Solomon, *Earth Planet. Sci. Lett.* **214**, 143 (2003).
21. G. Laske, J. Phipps Morgan, J. A. Orcutt, in *Plates, Plumes and Planetary Processes*, G. R. Foulger, D. M. Jurdy, Eds. (Special Paper 430, Geological Society of America, Boulder, CO, 2007), pp. 209–233.
22. J. A. Collins, F. L. Vernon, J. A. Orcutt, R. A. Stephen, *Geophys. Res. Lett.* **29**, 1522 (2002).
23. R. Katzman, L. Zhao, T. H. Jordan, *J. Geophys. Res.* **103**, 17933 (1998).
24. Materials and methods are available as supporting material on *Science* Online.
25. F. A. Dahlen, S.-H. Hung, G. Nolet, *Geophys. J. Int.* **141**, 157 (2000).
26. E. J. Garnero, T. Lay, A. McNamara, *Geol. Soc. Am. Spec. Paper* **430**, 79 (2007).
27. C. Herzberg *et al.*, *Geochem. Geophys. Geosyst.* **8**, Q02006 (2007).
28. M. A. Richards, R. W. Griffiths, *Geophys. J. Int.* **94**, 367 (1988).
29. P. E. van Keken, C. W. Gable, *J. Geophys. Res.* **100**, 7137 (1995).
30. W. H. F. Smith, D. T. Sandwell, *Science* **277**, 1956 (1997).

31. We are grateful to NSF for its support of this project. We thank G. Ito and M. Ballmer for helpful discussions, G. Nolet for input regarding methodology, and S. Grand for a copy of his global model. We also acknowledge the crews of the research vessels *Melville*, *Ka'imikai-O-Kanaloa*, and *Kilo Moana*; the *Jason* remotely operated vehicle team; the Ocean Bottom Seismograph Instrument Pool; the Carnegie Institution's portable seismology laboratory; and the hosts of temporary stations on the Hawaiian Islands. We thank L. Boschi and three anonymous reviewers for comments on earlier versions of this paper.

Supporting Online Material

www.sciencemag.org/cgi/content/full/326/5958/1388/DC1
Materials and Methods
SOM Text
Figs. S1 to S33
References

4 August 2009; accepted 8 October 2009
10.1126/science.1180165